Carbohydrate Polymers 218 (2019) 145–153

Contents lists available at ScienceDirect

Carbohydrate Polymers

journal homepage: www.elsevier.com/locate/carbpol

Low-energy preparation of cellulose nanofibers from sugarcane bagasse by modulating the surface charge density

Lidiane O. Pinto[a,b], Juliana S. Bernardes[a,*], Camila A. Rezende[b,*]

[a] Brazilian Nanotechnology National Laboratory (LNNano), Brazilian Center for Research in Energy and Materials (CNPEM), P.O. Box 6192, 13083-970, Campinas, SP, Brazil

[b] Institute of Chemistry, University of Campinas, P.O. Box 6154, 13083-970, Campinas, SP, Brazil

ARTICLE INFO

Keywords:
Cellulose nanofibers
Cellulose nanocrystals
TEMPO-mediated oxidation
Sugarcane bagasse
Eucalyptus chips

ABSTRACT

In this work, cellulose nanofibers (CNF) were obtained from sugarcane bagasse (SC) without high-energy mechanical treatments, using TEMPO-mediated oxidation. Variable NaClO concentrations were used to impart electrostatic repulsion between surface charged groups thus facilitating fibril separation. CNFs with diameters in the 3–5 nm range were obtained by oxidation of SC pulp with NaClO at 25 and 50 mmol/g. After a 30 min –sonication step, these CNFs were broken down into cellulose nanocrystals (CNC) by mechanical action. Both CNF and CNC preparation by this method are possible in SC due to its particular cell wall morphology and were not achieved in eucalyptus biomass, which is more recalcitrant. This work provided thus a new pathway to modulate the final morphology of cellulose particles by combining a low recalcitrant raw material with different surface charge densities.

1. Introduction

Over the last decade, there has been an increase in research on cellulose nanoparticles due to their outstanding properties, which includes high specific strength and stiffness, low density, high surface area, renewability, low toxicity and surface tunability by chemical modifications (Mondal, 2017). These nanoparticles have been investigated aiming at several applications, such as composite (Dufresne & Belgacem, 2010) and packing (Ghaderi, Mousavi, Yousefi, & Labbafi, 2014), foams (Ferreira & Rezende, 2018; Sain, Pan, Xiao, Farnood, & Faruk, 2013; Wicklein et al., 2015), sensor and devices (Liu, Sui, & Bhattacharyya, 2014; Rajala et al., 2016), emulsions (Gestranius, Stenius, Kontturi, Sjöblom, & Tammelin, 2017), rheology modifiers (Liu et al., 2017; Souza, Mariano, De Farias, & Bernardes, 2019), and biomedical devices (Lin & Dufresne, 2012; Liu et al., 2018; Poonguzhali, Khaleel Basha, & Sugantha Kumari, 2018; Supramaniam, Adnan, Mohd Kaus, & Bushra, 2018).

Based on morphological features, nanocelluloses can be categorized into two groups: cellulose nanocrystals (CNCs) and cellulose nanofibers (CNFs). CNCs are rod-like rigid particles with a diameter within the nanoscale and length of several hundred nanometers (Eichhorn, 2011). In turn, CNFs are long, flexible and entangled nanofibers, containing both crystalline and amorphous regions, with a diameter in nanoscale and length in microns (Kargarzadeh et al., 2018).

As a consequence of the compact and rigid structure of the lignocellulosic matrix, known as biomass recalcitrance, the production of both CNC and CNF requires harsh conditions (Rubin, Himmel, Ding, Johnson, & Adney, 2007). CNCs are obtained using pretreatments to isolate cellulose from the other biomass components, followed by hydrolysis with strong concentrated acids and dialysis for purification. Acid hydrolysis attacks amorphous cellulose regions, resulting in highly crystalline short particles with dimensions depending on the reaction conditions and on the cellulose source (Klemm et al., 2011).

On the other hand, to obtain CNFs, besides isolating cellulose, significant mechanical action is needed to separate neighboring cellulose nanofibrils, which are packed together *via* H-bonding among hydroxyl groups or physically entangled by single chain polysaccharides (Tejado, Alam, Antal, Yang, & van de Ven, 2012). Thus, refining (Karande, Bharimalla, Hadge, Mhaske, & Vigneshwaran, 2011), grinding (Iwamoto, Nakagaito, & Yano, 2007), and homogenization with homogenizers (Dufresne, 1999) or microfluidizers (Zimmermann, Pöhler, & Geiger, 2004), are common high-energy mechanical treatments used to isolate CNFs. Recently, there has been an intense research effort to produce nanocellulose under milder and more sustainable conditions (Chaker, Mutjé, Vilar, & Boufi, 2014; Jiang et al., 2018; Van Hai et al., 2018). In our research group, a method that combines the production of cellulose nanofibrils and nanocrystals by acid hydrolysis of elephant grass using 60% (m/m) H_2SO_4 was used. In the same

* Corresponding authors.
E-mail addresses: lidiane.pinto@iqm.unicamp.br (L.O. Pinto), juliana.bernardes@lnnano.cnpem.br (J.S. Bernardes), camila@iqm.unicamp.br (C.A. Rezende).

https://doi.org/10.1016/j.carbpol.2019.04.070
Received 11 January 2019; Received in revised form 13 March 2019; Accepted 19 April 2019
Available online 30 April 2019
0144-8617/

hydrolysis, CNC was obtained with a 12–16% w/w yield and CNF with a 4–10% w/w yield, depending on the previous pretreatments applied to the biomass (Nascimento & Rezende, 2018). In a second work, cellulose microfibers from eucalyptus pulp were partially hydrolyzed under milder conditions (H_2SO_4 48% w/w) to produce lightweight materials (0.15 g/cm^3), which were obtained by drying at low temperature (60 °C) in a convection oven, without the use of additives or special stirring equipment (Ferreira & Rezende, 2018).

Chemical and enzymatic treatments before the mechanical disintegration of the fibers are also strategies used by several researchers to minimize the energy input requirement, favoring CNF production on an industrial scale (Bahrami, Behzad, Zamani, Heidarian, & Nasri-Nasrabadi, 2018; Isogai, Saito, & Fukuzumi, 2011; Jiang et al., 2018; Kalia, Boufi, Celli, & Kango, 2014; Pääkko et al., 2007). These pretreatments can reduce the energy consumption from 20,000–30,000 kW h/ton to 1000 kW h/ton of biomass (Siró & Plackett, 2010). A promising chemical pretreatment consists of adding charges (carboxylate groups, COO^-) on the cellulose microfibril surface through oxidation procedures. Within these methods, TEMPO-mediated oxidation is particularly interesting, since it displays position-selective catalytic oxidation under moderate aqueous conditions, similar to enzymatic or biological reactions (Kalia et al., 2014; Saito, Kimura, Nishiyama, & Isogai, 2007).

Lately, a recent work (Zhou, Saito, Bergström, & Isogai, 2018) showed that TEMPO oxidation using high NaClO concentration (> 10 mmol/g) followed by 10–20 min of tip sonication could also be used to prepare CNCs from pinus and cotton fibers. Besides being an acid-free method, the CNCs produced had higher mass recovery than those extracted using conventional acid methods, thus opening new perspectives in nanocellulose research fields.

In the present study, TEMPO-mediated oxidation under an excess of oxidant agent (25 and 50 mmol/g) was applied to cellulose extracted from sugarcane bagasse (SC). This is a low recalcitrant biomass, inexpensive and available in large amounts in Brazil, which is the largest producer of sugarcane in the world. More than 630 million tons of this crop were cultivated in the 2017/2018 harvest (CONAB, 2017), of which one-third in weight corresponds to bagasse, an agricultural waste. CNCs were isolated from bleached sugarcane bagasse by Teixeira et al. using a traditional method also applied to other biomasses, based on acid hydrolysis with H_2SO_4 (6 M) at 45 °C for 30 min (Teixeira et al., 2011). In another work (de Campos et al., 2013), CNFs were obtained from bleached sugarcane bagasse with a combination of two enzymatic preparations (hemicell/pectinase and endoglucanase), followed by sonication for 20 min. Energy consumption was reduced in this work, without the normally used homogenization, but the mechanical process could not be completely eliminated.

Herein, TEMPO-oxidized cellulose nanofibers were extracted from sugarcane bagasse, avoiding the use of high-energy consuming procedures to promote mechanical defibrillation. Our hypothesis is that this method benefited from the low recalcitrant characteristics of sugarcane bagasse and the high charged densities imparted on cellulose surface by high concentrations of oxidant agent (NaClO 25–50 mmol/g substrate). We verified that the same oxidation procedure applied to a more structured and compact biomass, such as eucalyptus chips, did not result in defibrillation. We also hypothesize that TEMPO oxidation, besides charging the surface by the formation of carboxyl groups, removes lignin from cellulose fiber bundles in SC, which facilitates fiber disassembling due to the particular morphology of its plant cell wall. By sonication of previously oxidized bagasse samples, CNCs could also be obtained depending on the oxidation degree of the substrate, thus allowing a way to control the final morphology of the nanocellulose particles obtained.

2. Experimental section

2.1. Materials

Sugarcane bagasse (SC) and eucalyptus chips (E) were obtained from CTBE (Brazilian Bioethanol Science and Technology Laboratory, Campinas-SP, Brazil) and Fibria (São Paulo-SP, Brazil), respectively. Bagasse fibers had an average length of 6 ± 5 mm and an average diameter of 0.3 ± 0.2 mm. Eucalyptus chips were typically shorter (average length of 2.5 ± 0.9 mm) and wider (average diameter of 0.8 ± 0.5 mm) than bagasse fibers. More information about the morphology of sugarcane bagasse and eucalyptus chips (including optical and scanning electron microscopies, measurements of cell wall thickness, lumen diameter and histograms of size distributions) can be found in the Supplementary material (Figs. S1–S5 and Table S1). Sodium hydroxide, hydrogen peroxide, 2,2,6,6-tetramethylpiperidine-1-oxyl (TEMPO) and sodium borohydride were purchased from Sigma-Aldrich and sodium hypochlorite (12% w/v) from Star Flash.

2.2. Isolation of cellulose nanofibers (CNFs) and cellulose nanocrystals (CNCs)

CNFs and CNCs with carboxyl functional groups on the surface were isolated from sugarcane bagasse after organosolv, bleaching and TEMPO oxidation pretreatments, as schematically represented in Fig. 1. Eucalyptus chips underwent the same experimental procedure to evaluate the effect of the raw material on the isolation of nanocelluloses.

2.2.1. Organosolv pulping

In this pretreatment, 300 g of sugarcane bagasse were treated with a 1:1 (v/v) ethanol/water solution at a 1:10 solid to liquid ratio in a PARR reactor at 190 °C for 2 h, as previously described (de Oliveira, Bras, Pimenta, da S. Curvelo, & Belgacem, 2016). The resulting pulp was mixed with a 1% (w/w) NaOH solution and rinsed with water until achieving neutral pH.

2.2.2. Pulp bleaching

This procedure was adapted from a previous method (Teixeira et al., 2011). The dry pulp (40 g) was suspended in 800 mL of a 5% (w/w) NaOH solution at 70 °C. Then, 800 mL of hydrogen peroxide (24% w/w in water) was slowly added to the suspension and the system was mechanically stirred at 500 rpm for 40 min. Bleached pulp was then separated by filtration, rinsed with water until neutral pH, and the bleaching step was repeated.

2.2.3. TEMPO-mediated oxidation

Bleached fibers were oxidized using TEMPO-mediated oxidation in water at pH 10 (Isogai et al., 2011). Sugarcane bagasse or eucalyptus cellulose fibers (5 g) were hydrated in ultrapure water (500 mL) for 24 h, followed by the addition of TEMPO (0.08 g, 0.5 mmol) and sodium bromide (0.5 g, 5 mmol). Then, oxidation started by the addition of specific volumes (15.6 or 78.0 or 156.0 mL per gram of cellulose) of a 12% (w/v) NaClO solution. The initial pH of this NaClO solution was around 11–12 and it was adjusted to 10 by adding a 0.1 M HCl solution before the addition to the fiber suspension. The bleached fibers were stirred at room temperature by a propeller stirrer (QUIMIS) at 200 rpm, while pH 10 was maintained by adding 0.5 M NaOH until no more NaOH consumption was detected by a MARCONI pH meter (*ca.* 130 min). Finally, TEMPO-oxidized cellulose was abundantly rinsed with ultrapure water by centrifugation until constant conductivity was reached in water, monitored by an AJX-515 conductometer (AJMICRONAL). Oxidized samples obtained from sugarcane bagasse (SC) or eucalyptus (E) were identified as SC-5, SC-25 and SC-50 or E-5, E-25 or E50, depending on the concentration of NaClO used in the reaction (5, 25 or 50 mmol/g substrate). A fraction of each sample was vacuum-dried at 60 °C for 24 h and weighed to measure the mass recovery ratios.

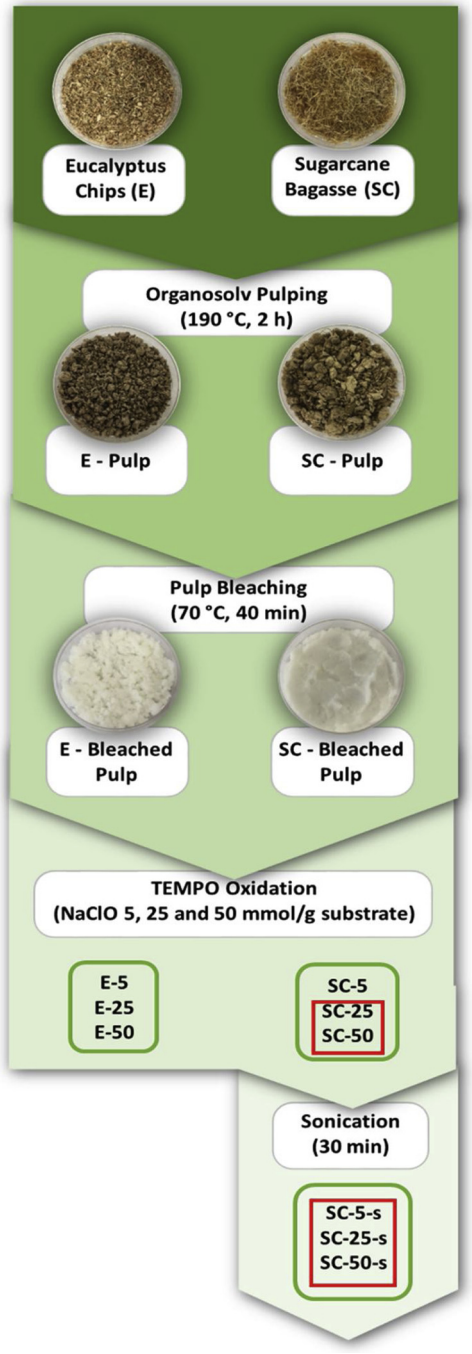

Fig. 1. Procedure to isolate nanocelluloses (CNFs and CNCs) from sugarcane bagasse and eucalyptus chips, including organosolv pulping as pretreatment, bleaching and TEMPO oxidation. Sonication was carried out in bagasse samples only. Samples at the nanoscale are delimited by the red square. (For interpretation of the references to colour in this figure legend, the reader is referred to the web version of this article).

2.2.4. Mechanical fibrillation

Nanofibrillation of TEMPO-oxidized cellulose was performed using a 130-W ultrasonication system (Vibra-Cell VCX130), at a 40% oscillation amplitude (Mishra, Manent, Chabot, & Daneault, 2012). The samples (0.5 g) were suspended in distilled water (50 mL) and sonicated for 30 min in an ice bath. After sonication, TEMPO-oxidized samples were identified with the index "s" (Fig. 1).

2.3. Sample characterization

TEMPO-oxidized celluloses before and after sonication were dispersed in water to obtain final concentrations of 0.1% and 0.0005% w/w to optical and atomic force microscopy (AFM) analyses, respectively. Then, the dispersions were dropped in silica substrates for optical microscopy or cleaved mica supports for AFM characterization, and the substrates were allowed to dry by natural evaporation.

Optical microscopy images were obtained in the Zeiss Escope.A1 reflection optical microscope equipped with EC EPIPLAN 10x/0,25 HD lens. AFM images were obtained in the Park NX 10 equipment, in non-contact mode, using silicon tips (FMR NanoWorld), with cantilever spring constant of 2.8 N/m and nominal resonance of 75 kHz.

Transmittance measurements of samples after sonication (3% w/w) were carried out in a Biochrom Spectrophotometer (Libra) model S70 at 600 nm, using a semi-micro disposable polystyrene cuvette.

X-ray photoelectron spectroscopy (XPS) analyses were recorded with a Thermo K-Alpha (Thermo Scientific, Inc.) equipment, with a monochromatic Al Kα X-ray (1486.7 eV) source. All survey spectra were obtained with pass energy of 200 eV and short scan spectra of 50 eV.

Conductometric titration was used to determine the carboxyl content on the surface of oxidized cellulose, as previously described (Lin & Dufresne, 2012). Samples (50 mg) were suspended in 15 mL of a 0.01 M hydrochloric acid solution and 75 mL of water. After 10 min stirring, the suspension was titrated with 0.01 M NaOH.

The quantification of cellulose and hemicellulose was performed in solid samples of bleached sugarcane bagasse and eucalyptus chips, as previously described (Rezende et al., 2011). Samples were hydrolyzed in H_2SO_4 72% w/w and the hydrolysate was separated from the residual solid by filtration. Ash contents were determined as the inorganic residue remaining after complete calcination of the solid fraction in a muffle at 800 °C. The hydrolysate material was filtered in a syringe filter (Analitica, pore diameter 0.22 nm) and used in the determination of hydrolysed sugars. This process was carried out in duplicate by high performance liquid chromatography (HPLC) in an Agilent series 1200 equipment, with a refractive index detector and an Aminex column (HPX-87H, 300 × 7.8 mm, Bio-Rad, Hercules-CA, USA), at 45 °C, using a 5 mM H_2SO_4 solution as mobile phase at a 0.6 mL/min flow rate. Acetyl bromide soluble lignin was also determined in sugarcane bagasse and eucalyptus samples, as described elsewhere (Moreira-Vilar et al., 2014) (ref).

3. Results and discussion

3.1. Overview of tempo-oxidized celluloses

TEMPO/NaBr/NaClO oxidation applied to cellulose pulps at pH 10 and room temperature is capable to convert significant amounts of C6 primary hydroxyl groups to sodium carboxylates. The introduction of anionically charged COO^- groups promotes strong electrostatic repulsion between cellulose fibrils in water, favoring their defibrillation with mechanical disintegration treatments (Isogai et al., 2011). To investigate the effect of oxidation degree on the isolation of nanocelluloses from sugarcane bagasse, we varied the NaClO concentration (5, 25 or 50 mmol/g substrate). When the added amounts of NaClO were 25 or 50 mmol/g (SC-25 or SC-50), cellulose pulps showed less turbidity than when using 5 mmol/g (SC-5, Fig. 2a). Besides this, we observed that SC-25 and SC-50 (3% w/w) are viscous samples and when the vials were inverted (Fig. 2b), SC-50 did not flow for at least 30 min, forming an invertible gel, which is an evidence of fiber fibrillation. Dispersions of cellulose nanofibers become a gel at very low concentrations because of the high degree of entanglements and crosslinking points of partially disintegrated fiber aggregates. The networks are inherent, and gels are stronger than when the network is formed *via* hydrogen bonds, such as in CNC gels (Pääkko et al., 2007).

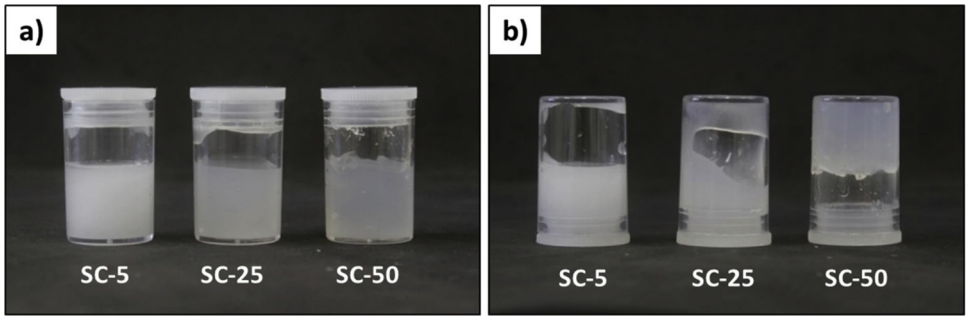

Fig. 2. Photographs of TEMPO-oxidized cellulose dispersions from sugarcane bagasse (3% w/w), using different NaClO concentrations (5, 25 or 50 mmol/g for SC-5, SC-25 and SC-50, respectively): (a) before and (b) after vial inversion tests.

On the other hand, when eucalyptus was used as starting material, the three oxidized cellulose pulps presented similar features under visual inspection, regardless of the NaClO concentration (Fig. S6 in the Supplementary material). Eucalyptus samples were turbid and less viscous as SC-5, and they did not form invertible gels, indicating that the cellulose fibers were not disassembled into nanoparticles in this case. This visual observation of gel flow behavior is a first evidence of eucalyptus higher recalcitrance as compared to sugarcane bagasse.

To understand the microstructure of the cellulosic materials after oxidation, we first analyzed the dried samples by optical microscopy. Fig. 3 shows that the oxidized celluloses produced from sugarcane bagasse or eucalyptus chips at mild conditions (SC-5 and E-5) have the same morphological aspects: microfibers involved by a dried thin film. These microfibers are non-fibrillated remnants of the fibers imaged by optical and scanning electron microscopy in samples *in natura* (Supplementary material, Figs. S1, S3 and S4).

By increasing the amount of NaClO, optical microscopy images allowed the identification of a progressive reduction in the number of microfibers for SC-25 and SC-50 samples (Fig. 3a). On the other hand, the changes in NaClO concentration did not alter the morphology of celluloses from eucalyptus chips. In Fig. 3b, samples E-25 and E-50 maintain their aspect with microfibers involved by a dried film, just as in sample E-5.

The mass recovery ratio is an indication of solubilization of cell wall components and of the process severity. In TEMPO-oxidized pulps, the mass recovery varied according to the raw material and the NaClO concentration (Table 1). In SC-5, 94% of the solid remained after the reaction, while SC-25 and SC-50 were not recovered as solids in high yields (57 and 59%, respectively). Differently, eucalyptus pulps presented similar yields independently of the NaClO concentration (78%, 79% and 83% for E-5, E-25 and E-50, respectively). Water-soluble molecules were probably formed under higher oxidant contents in SC cellulose samples (SC-25 and SC-50), and were leached during the washing process (Tejado et al., 2012). Eucalyptus samples did not show the same solubilization levels as SC, presenting similar mass recovery ratios for all the samples (around 80%) under different NaClO concentrations.

Table 1
Mass recovery ratio, transmittance, width and length of sugarcane bagasse nanoparticles obtained after oxidation.

Sample	Mass recovery ratio (%)	Transmittance (%)[a]	Nanoparticle Width (nm)	Nanoparticle Length (nm)
SC-5	94	–	[b]	[b]
SC-5-s	–	2.50	4 ± 2	605 ± 170
SC-25	57	–	4 ± 1	379 ± 132
SC-25-s		58.5	4 ± 1	194 ± 87
SC-50	59	–	4 ± 1	243 ± 119
SC-50-s		61.4	4 ± 1	159 ± 71

[a] Transmittance measured for 3% w/w cellulose dispersions at 600 nm.
[b] Width and length of nanostructures were not measured for sample SC-5 because microfibers were not defibrillated.

Transmittance and flow characteristics, together with mass recovery and optical microscopy results of SC microfibers oxidized at increasing

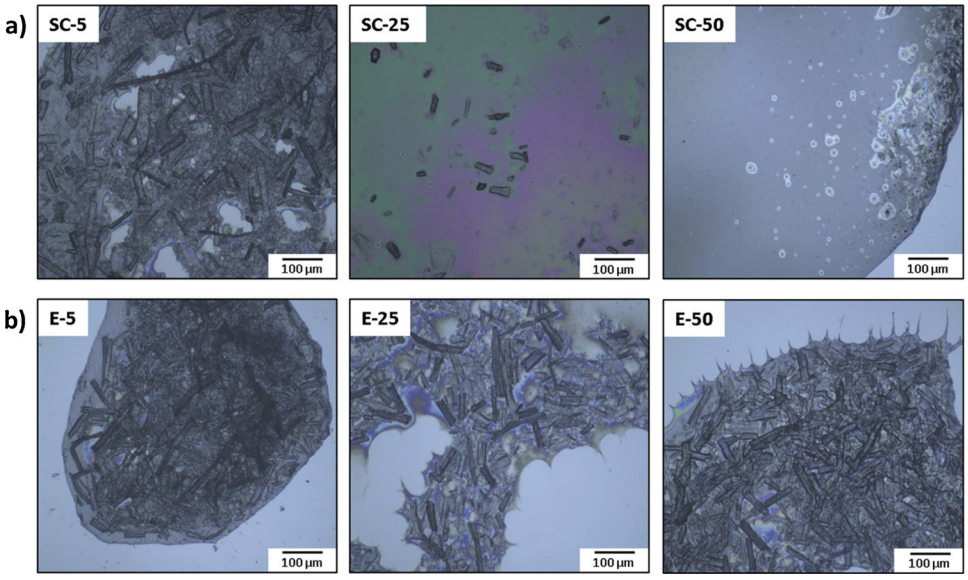

Fig. 3. Optical microscopy images of TEMPO-oxidized cellulose pulps from (a) sugarcane bagasse (SC) and (b) eucalyptus chips (E).

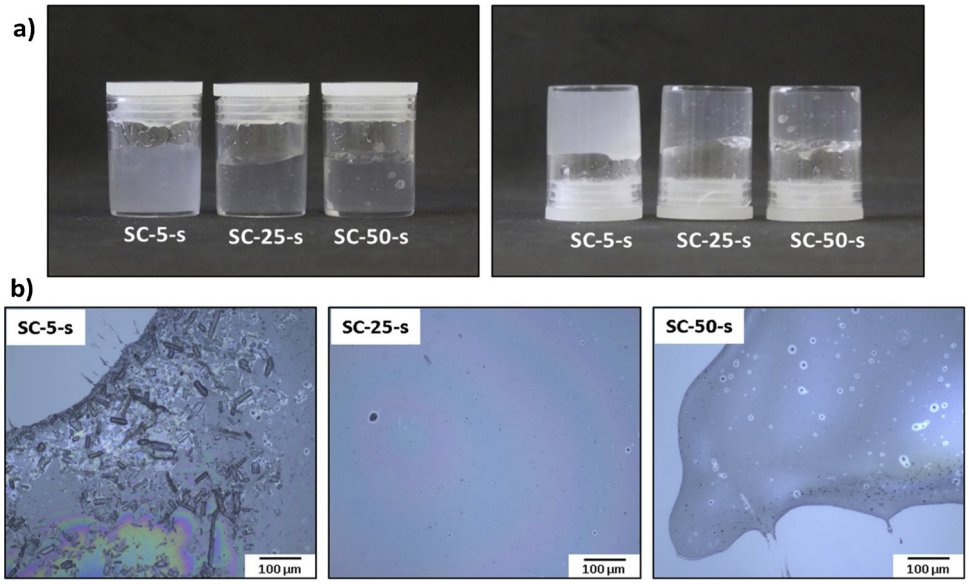

Fig. 4. (a) Photographs and (b) optical microscopy images of TEMPO-oxidized cellulose pulps from sugarcane bagasse (SC) after sonication.

NaClO concentrations suggest that they had been disassembled into nanostructures. Indeed, these results were confirmed by atomic force microscopies (AFM) of the nanostructures contained in the solid film involving the nanoparticles (Fig. 5).

TEMPO-oxidized pulps from sugarcane (1% w/w) were also treated by sonication for 30 min to reduce the dimensions of the isolated fibers. In fact, the small amount of microfibers presented in sample SC-25 (Fig. 3a) were no longer observable after sonication (SC-25-s in Fig. 4b). Also, the number of visible microfibers in sample SC-5 (Fig. 3a) was drastically reduced after mechanical disintegration (SC-5-s in Fig. 4b). Besides this, the turbidity of the dispersions (Fig. 4a) decreased after sonication, as compared to the non-sonicated ones (Fig. 2a). The light transmittance at 600 nm for 3% (w/w) dispersions rised from 2.5 to *ca.* 60% when the NaClO concentration increased from 5 to 25 and 50 mmol/g (Table 1). All the samples also formed invertible gels after sonication (Fig. 4a), which indicates the possible self-assembly of the nanoparticles into a nematic phase, as will be detailed in a following section.

AFM topography images of oxidized celluloses from sugarcane bagasse (Fig. 5) were obtained in the transparent films involving the microfibers in Figs. 3a and 4b to evaluate the presence of structures in the nanometer scale, not visible by optical microscopy. Prior to sonication (Fig. 5a), the sample prepared at mild oxidant content (SC-5) presented aggregated fibril bundles, as already observed for different types of biomass, like wood, sugar beet or potato tuber (Klemm et al., 2011).

By increasing the oxidation degree (SC-25 and SC-50), most of the cellulosic fibers disaggregate without the need for high-energy mechanical treatments, such as sonication or high-pressure homogenization (Fig. 5). These samples have characteristic features of nanofibers, presenting kinks and a relatively constant cross-section with average widths in the range of 3–5 nm (Table 1), which may correspond to elementary fibril dimensions, based on Ding and Himmel's model for maize biomass (Ding & Himmel, 2006).

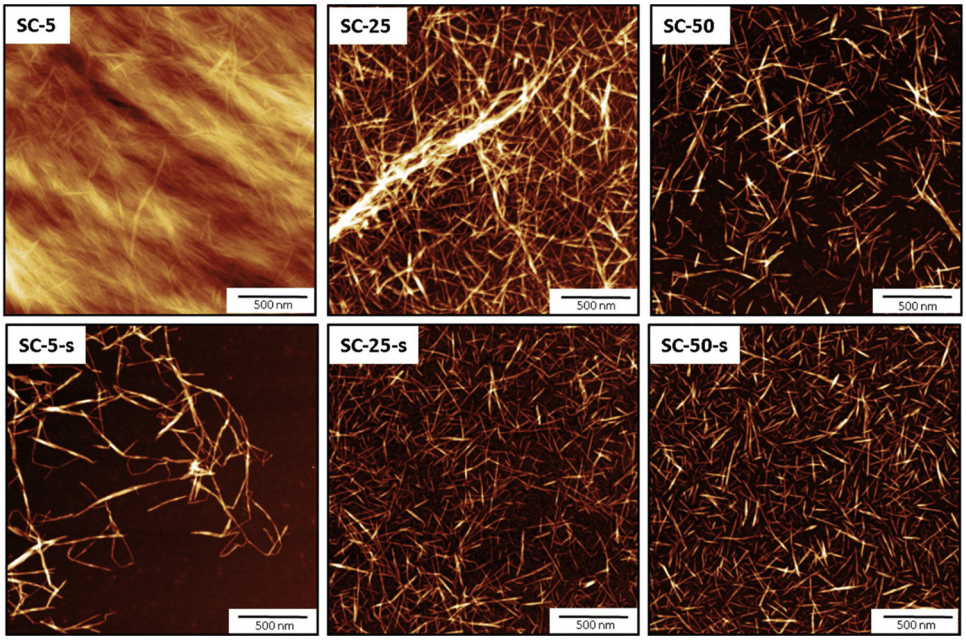

Fig. 5. Topography AFM images of TEMPO-oxidized celluloses from sugarcane pulp oxidized under different amounts of NaClO (a) before and (b) after sonication.

Besides that, the length of these nanoelements reduced when charge density increased (Table 1). This suggests that the oxidation mediated by TEMPO, in addition to disassembling the bundles, also promoted a perpendicular cleavage in the fibers (Fig. 5). After sonication, cellulose fibers of sample SC-5 are partially disintegrated without complete individualization (SC-5-s in Fig. 5). These results reveal that harsh oxidation (SC-25 and SC-50) is more efficient to fragment cellulose sheets from sugarcane bagasse along their length than the mild oxidation/sonication combined approach.

The sonication of cellulose pulps with a high oxidation degree (SC-25-s and SC-50-s) led to the formation of needle-like particles (CNC) shown in Fig. 5 and as recently observed by Isogai in microcrystalline cellulose and bleached Kraft pulp (Zhou et al., 2018). The length of the particles reduced considerably, while the width (*ca.* 4 nm) was not altered, suggesting that, in most of the cases, the mechanical treatment was not able to break the fibrils in units with a diameter smaller than the one of the elementary fibril. (Li & Renneckar, 2010; Wang et al., 2012)

The final morphology of the oxidized samples can also be correlated to the mass recovery ratios reported in Table 1. Sample SC-5, which has only 6% of its weight solubilized (Table 1), maintains its morphology of fiber bundle in Fig. 5. On the other hand, the defibrillation in SC-25 and the further breaking down of the nanofibrils in SC-50 (Fig. 5) is followed by solubilization of *ca.* 40% of the substrate components. Crystallinity index (CI) values were also calculated for these samples using the height method based on x-ray diffraction patterns (Segal, Creely, Martin, & Conrad, 1959). A detailed description of these analyses can be found in the Supplementary material (Figs. S7–S8 and Table S2). IC increases from 64% in SC-5 (packed fibrils in Fig. 5) to 73% in SC-25 (formed by individual fibrils) and to 77% in SC-50 (nanocrystals). Crystallinity results indicate the removal of amorphous fractions from these samples, mainly residual lignin and amorphous cellulose, and are in accordance with the mass recovery data.

3.2. Chemical characterization

Table 2 shows the compositional analysis of sugarcane bagasse and eucalyptus bleached pulps (the step immediately prior to oxidation) in terms of lignin, cellulose, hemicellulose and ash contents.

Bleached SC is slightly poorer in cellulose and a little richer in hemicellulose than bleached eucalyptus. Lignin percentages are very similar in these two bleached biomasses, so that the higher susceptibility of sugarcane bagasse to the breaking down of their microfibers into nanofibrils by oxidation (micrographs in Figs. 3 and 5) can not be assigned to its lignin content. Other causes should be thus investigated, such as the degree of oxidation and the oxygen to carbon ratio in these samples.

Acethyl bromide lignin was also determined in SC-in natura and in SC-pulp, and a significant decrease in the lignin content from 27.0 ± 2.0% to 7.7 ± 0.7% was observed in the pulping process (Supplementary material, Table S2). After bleaching, the lignin amount is further reduced as can be observed in Table 2. Lignin could not be quantified in oxidized samples, since the common methods used for this purpose (Klason and acetyl bromide lignin) do not provide reliable results in samples with high amounts of crystalline cellulose and with very low amounts of lignin.

TEMPO-mediated oxidation selectively oxidizes the accessible alcohol group in C6 to aldehyde and ionizable carboxylic groups

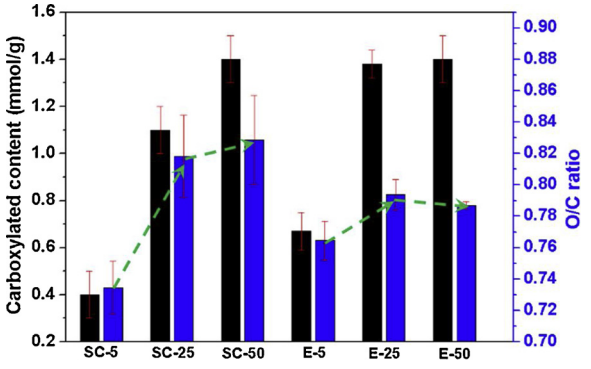

Fig. 6. Carboxylate content (black) and O/C ratio (blue) for sugarcane and eucalyptus oxidized celluloses prepared with different NaClO concentrations (mmol/g substrate) (For interpretation of the references to colour in this figure legend, the reader is referred to the web version of this article).

(COO^-Na^+) (Saito et al., 2007). Therefore, the degree of oxidation (DS) of SC-5, SC-25 and SC-50 was investigated by conductometric titration, yielding gravimetrically normalized values of 0.40; 1.07 and 1.40 mmol/g, respectively (Fig. 6). DS of celluloses from eucalyptus presented similar results (0.67; 1.38 and 1.40 mmol/L for samples E-5, E-25 and E-50, respectively). So, again, this result alone can not explain the different susceptibility of SC and eucalyptus to defibrillation.

Oxygen to carbon ratio (O/C in Fig. 6, calculated from XPS Survey Spectra) showed a more pronounced increase in sugarcane bagasse when the NaClO concentration increased from 5 to 25 and 50 mmol/g, as compared to eucalyptus samples. These results suggest that a severe oxidation step (NaClO 25 or 50 mmol/g), besides promoting the addition of oxygenated groups on the bagasse surface, has also removed carbon-rich compounds.

According to previous reports, TEMPO-mediated oxidation is able to remove lignin from pretreated lignocellulosic pulps, apart from oxidizing them (Ma, Fu, Zhai, Law, & Daneault, 2012; Rahimi, Azarpira, Kim, Ralph, & Stahl, 2013). Additionally, sugarcane bagasse is known to present significant defibrillation of its microfiber bundles when undergoing delignification processes (Rezende et al., 2011; Yue et al., 2015). The combined action of lignin removal and the increase in surface charge density would be the cause for the efficiency of the proposed method when applied to sugarcane biomass.

Comparing previous works of this research group on delignification of sugarcane bagasse (Rezende et al., 2011) and eucalyptus bark (Lima et al., 2013) using NaOH solutions, the much more recalcitrant profile of eucalyptus is evidenced. While NaOH solutions at 2 and 4% w/v (120 °C and 1.05 bar for 40 min) caused significant defibrillation of microfiber bundles in the bagasse cell wall, the same pretreatment conditions for 1 h had only a superficial action on eucalyptus chips and were not able to completely separate the cell wall fibers completely.

Easier defibrillation in sugarcane bagasse can be assigned to a particular distribution of lignin domains in its cell wall, present in the interstices of the fiber bundles and attaching the cellulose fibers longitudinally to each other (Fromm, Rockel, Lautner, Windeisen, & Wanner, 2003; Rezende et al., 2011). The removal of this lignin by any delignification process, TEMPO-oxidation for instance, would dismantle the structure of the bundles and result in more independent fibers. Eucalyptus substrates, conversely, are much more recalcitrant to defibrillation under delignification, due to the morphological aspects of

Table 2
Acetyl bromide soluble lignin, cellulose, hemicellulose, ash contents and mass closure for bleached pulps of sugarcane bagasse and eucalyptus.

Beached samples	Acetyl bromide lignin (%)	Cellulose (%)	Hemicellulose (%)	Ash (%)	Mass closure (%)
Sugarcane bagasse	3.5 ± 0.5	86.0 ± 1.0	7.62 ± 0.07	0.86 ± 0.03	98.6 ± 1.1
Eucalyptus chips	2.8 ± 0.4	90.3 ± 0.2	4.89 ± 0.03	0.51 ± 0.03	98.5 ± 0.5

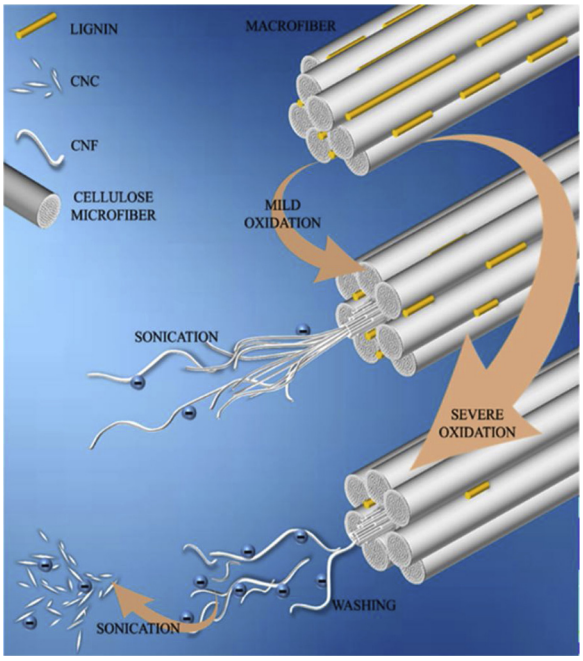

Fig. 7. Proposed model of oxidation action in sugarcane bagasse microfibers under mild (5 mmol NaClO/g substrate) or severe (25 or 50 mmol NaClO/g substrate) conditions.

their cell walls.

Based on previous knowledge about lignin distribution in SC fiber bundles and also on TEMPO ability to remove lignin from plant cell walls, the following model is proposed to explain the different morphological features in nanocelluloses obtained under different conditions of oxidation and sonication (Fig. 7). Under mild oxidation (NaClO, 5 mmol/g), residual lignin is not efficiently extracted, and the fiber surface remained poorly charged, so that defibrillation of microfiber bundles only occurred after high-intensity sonication treatment. On the other hand, by using severe oxidation (NaClO, 25 or 50 mmol/g), residual lignin is efficiently removed, and the surface became highly charged. The outcome is that the elementary fibrils are released during the washing step without the need for any high-energy procedures. The sonication of these cellulose pulps led to the formation of needle-like particles (CNC), dismissing the use of concentrated acids, as generally required in the traditional acid hydrolysis.

Evidence of lignin removal was obtained from XPS (increase in O/C ratio) and XRD (IC increase from SC-5 to SC-50). Though lignin removal could be accurately quantified from samples *in natura* to the bleached ones, the methods to quantify residual lignin are not effective for lignin amounts so small (lower than 3.5%).

3.3. Self-assembly of cellulose nanoparticles

TEMPO-CNC nanoparticles have a lower width (*ca.* 4 nm) than those prepared by conventional sulfuric acid hydrolysis (4–20 nm) (Moon, Martini, Nairn, Simonsen, & Youngblood, 2011) and self-assemble into an anisotropic nematic phase as the suspension is concentrated by ambient evaporation (Fig. 8). At low solid content (1% w/w), SC-25-s and SC-50-s samples were low viscous and isotropic when observed between crossed polarizers. As the TEMPO-CNC content increased to 1.5% w/w, the samples became highly viscous and formed an anisotropic phase (birefringent).

Compared to CNCs prepared by sulfuric acid hydrolysis, TEMPO-CNCs investigated here are fully anisotropic at a much lower solid concentration (1.5% against 6–7% w/w for sulfonated CNCs) due to the higher charge density: 0.20 *versus* 1.1–1.4 mmol of charges per gram for sulfate-CNC and TEMPO-CNCs, respectively (Lokanathan, Uddin, Rojas, & Laine, 2014). This is consistent with Onsager's theory, which proposes that the isotropic-anisotropic phase transition for charged particles depends mainly on the electrical double layer and less on the physical particle size (Azizi Samir, Alloin, & Dufresne, 2005).

For both CNC-TEMPO systems (SC-25s and SC-50-s), the coexistence of isotropic and anisotropic phases that takes place spontaneously in sulfonated CNC suspensions was not detected, probably because this is a narrow region in the phase diagram. The self-assembly property of CNC-TEMPO are promising to produce new functional materials, transferring chiral nematic patterns to other solid compounds.

4. Conclusion

The method used in this work to prepare nanocellulose from sugarcane bagasse biomass resulted in cellulose nanofibers using TEMPO-mediated oxidation under increasing amounts of NaClO (from 5 to 25 and 50 mmol/g substrate) and without a mechanical defibrillation step. The addition of an excess of negative charges on the fiber surface and the removal of lignin by oxidation both contributed to fibrillation and consequently to the isolation of elementary fibrils, with widths in the range of 3–5 nm. Eucalyptus pulp under the same procedures did not present the same behavior due to their recalcitrant profile. Sonication of samples with a higher oxidation degree led to a perpendicular cleavage of the elementary fibers, obtaining cellulose nanocrystals with high mass recovery, without an acid hydrolysis process.

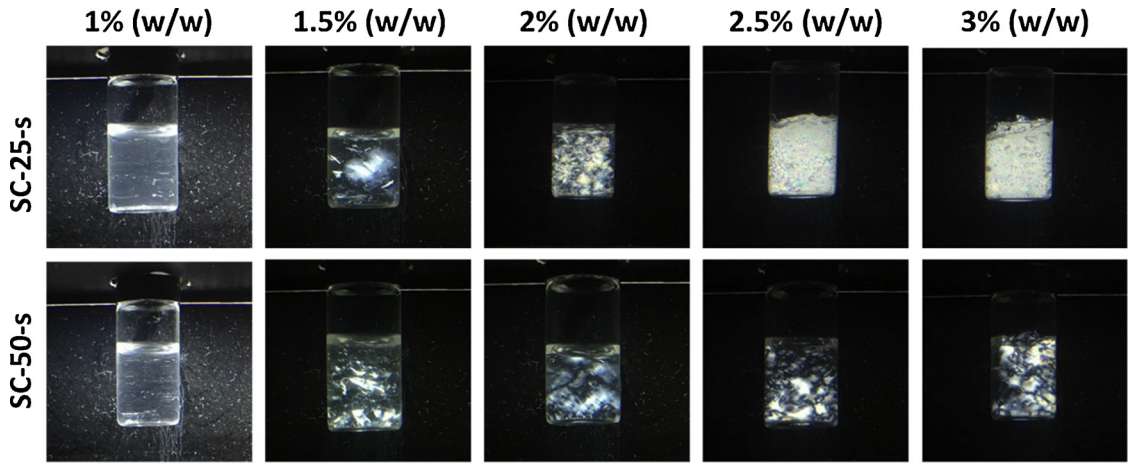

Fig. 8. Photographs of TEMPO-CNCs dispersions of SC-25-s and SC-50-s at different concentrations acquired between crossed polarizers after 7 day equilibration.

Acknowledgments

The authors thank the Brazilian Federal Agency for Support and Evaluation of Graduate Education within the Ministry of Education of Brazil (CAPES, by L.O.P Scholarship); the São Paulo Research Foundation (FAPESP, Grants No. 2016/04514-7 and 2016/13602-7) for research funding; and Espaço da Escrita – Pró-Reitoria de Pesquisa – UNICAMP for the language services provided.

Appendix A. Supplementary data

Supplementary material related to this article can be found, in the online version, at doi:https://doi.org/10.1016/j.carbpol.2019.04.070.

References

Azizi Samir, M. A. S., Alloin, F., & Dufresne, A. (2005). Review of recent research into cellulosic whiskers, their properties and their application in nanocomposite field. *Biomacromolecules, 6*(2), 612–626. https://doi.org/10.1021/bm0493685.

Bahrami, B., Behzad, T., Zamani, A., Heidarian, P., & Nasri-Nasrabadi, B. (2018). Optimal design of ozone bleaching parameters to approach cellulose nanofibers extraction from sugarcane bagasse fibers. *Journal of Polymers and the Environment, 26*(10), 4085–4094. https://doi.org/10.1007/s10924-018-1277-5.

Chaker, A., Mutjé, P., Vilar, M. R., & Boufi, S. (2014). Agriculture crop residues as a source for the production of nanofibrillated cellulose with low energy demand. *Cellulose, 21*(6), 4247–4259. https://doi.org/10.1007/s10570-014-0454-5.

CONAB (2017). *Perfil do Setor do Açúcar e do Etanol no Brasil - safra 2014/2015.* 64 https://doi.org/ISSN2318-3772.

de Campos, A., Correa, A. C., Cannella, D., de, M., Teixeira, E., Marconcini, J. M., et al. (2013). Obtaining nanofibers from curauá and sugarcane bagasse fibers using enzymatic hydrolysis followed by sonication. *Cellulose, 20*(3), 1491–1500. https://doi.org/10.1007/s10570-013-9909-3.

de Oliveira, F. B., Bras, J., Pimenta, M. T. B., da S. Curvelo, A. A., & Belgacem, M. N. (2016). Production of cellulose nanocrystals from sugarcane bagasse fibers and pith. *Industrial Crops and Products, 93*, 48–57. https://doi.org/10.1016/j.indcrop.2016.04.064.

Ding, S. Y., & Himmel, M. E. (2006). The maize primary cell wall microfibril: A new model derived from direct visualization. *Journal of Agricultural and Food Chemistry, 54*(3), 597–606. https://doi.org/10.1021/jf051851z.

Dufresne, A. (1999). Cellulose microfibrils from potato tuber cells: Processing and characterization of starch – Cellulose microfibril composites. *Journal of Applied Polymer Science, 76*(14), 2080–2092.

Dufresne, A., & Belgacem, M. N. (2010). Cellulose-reinforced composites: From micro-to nanoscale. *Polímeros Ciência e Tecnologia, 20*(1), 1–10. https://doi.org/10.4322/polimeros.2010.01.001.

Eichhorn, S. J. (2011). Cellulose nanowhiskers: Promising materials for advanced applications. *Soft Matter, 7*(2), 303–315. https://doi.org/10.1039/c0sm00142b.

Ferreira, E. S., & Rezende, C. A. (2018). Simple preparation of cellulosic lightweight materials from Eucalyptus pulp. *ACS Sustainable Chemistry & Engineering, 6*, 14365–14373. https://doi.org/10.1021/acssuschemeng.8b03071 research-article.

Fromm, J., Rockel, B., Lautner, S., Windeisen, E., & Wanner, G. (2003). Lignin distribution in wood cell walls determined by TEM and backscattered SEM techniques. *Journal of Structural Biology, 143*(1), 77–84. https://doi.org/10.1016/S1047-8477(03)00119-9.

Gestranius, M., Stenius, P., Kontturi, E., Sjöblom, J., & Tammelin, T. (2017). Phase behaviour and droplet size of oil-in-water Pickering emulsions stabilised with plant-derived nanocellulosic materials. *Colloids and Surfaces A: Physicochemical and Engineering Aspects, 519*, 60–70. https://doi.org/10.1016/j.colsurfa.2016.04.025.

Ghaderi, M., Mousavi, M., Yousefi, H., & Labbafi, M. (2014). All-cellulose nanocomposite film made from bagasse cellulose nanofibers for food packaging application. *Carbohydrate Polymers, 104*(1), 59–65. https://doi.org/10.1016/j.carbpol.2014.01.013.

Isogai, A., Saito, T., & Fukuzumi, H. (2011). TEMPO-oxidized cellulose nanofibers. *Nanoscale, 3*(1), 71–85. https://doi.org/10.1039/C0NR00583E.

Iwamoto, S., Nakagaito, A. N., & Yano, H. (2007). Nano-fibrillation of pulp fibers for the processing of transparent nanocomposites. *Applied Physics A: Materials Science & Processing, 89*(2), 461–466. https://doi.org/10.1007/s00339-007-4175-6.

Jiang, Y., Li, K., Wang, S., Qin, C., Yang, S., Liu, X., et al. (2018). Enzyme-assisted mechanical grinding for cellulose nanofibers from bagasse: Energy consumption and nanofiber characteristics. *Cellulose, 25*(12), 7065–7078. https://doi.org/10.1007/s10570-018-2071-1.

Kalia, S., Boufi, S., Celli, A., & Kango, S. (2014). Nanofibrillated cellulose: Surface modification and potential applications. *Colloid and Polymer Science, 292*(1), 5–31. https://doi.org/10.1007/s00396-013-3112-9.

Karande, V. S., Bharimalla, A. K., Hadge, G. B., Mhaske, S. T., & Vigneshwaran, N. (2011). Nanofibrillation of cotton fibers by disc refiner and its characterization. *Fibers and Polymers, 12*(3), 399–404. https://doi.org/10.1007/s12221-011-0399-3.

Kargarzadeh, H., Mariano, M., Gopakumar, D., Ahmad, I., Thomas, S., Dufresne, A., et al. (2018). Advances in cellulose nanomaterials. *Cellulose, 25*(4), 2151–2189. https://doi.org/10.1007/s10570-018-1723-5.

Klemm, D., Kramer, F., Moritz, S., Lindström, T., Ankerfors, M., Gray, D., et al. (2011). Nanocelluloses: A new family of nature-based materials. *Angewandte Chemie - International Edition, 50*(24), 5438–5466. https://doi.org/10.1002/anie.201001273.

Li, Q., & Renneckar, S. (2010). Supramolecular structure characterization of molecularly thin cellulose I nanoparticles. *Biomacromolecules, 12*(3), 650–659. https://doi.org/10.1021/bm101315y.

Lima, M. A., Lavorente, G. B., Da Silva, H. K. P., Bragatto, J., Rezende, C. A., Bernardinelli, O. D., et al. (2013). Effects of pretreatment on morphology, chemical composition and enzymatic digestibility of eucalyptus bark: A potentially valuable source of fermentable sugars for biofuel production – Part 1. *Biotechnology for Biofuels, 6*(1), 1–17. https://doi.org/10.1186/1754-6834-6-75.

Lin, N., & Dufresne, A. (2012). TEMPO-oxidized nanocellulose participating as cross-linking aid for alginate-based sponges. *Appl. Mater. Interfaces, 4*(9), 4948–4959. https://doi.org/10.1021/am301325r.

Liu, C., Du, H., Dong, L., Wang, X., Zhang, Y., Yu, G., et al. (2017). Properties of nanocelluloses and their application as rheology modifier in paper coating. *Industrial & Engineering Chemistry Research, 56*(29), 8264–8273. https://doi.org/10.1021/acs.iecr.7b01804.

Liu, D. Y., Sui, G. X., & Bhattacharyya, D. (2014). Synthesis and characterisation of nanocellulose-based polyaniline conducting films. *Composites Science and Technology, 99*, 31–36. https://doi.org/10.1016/j.compscitech.2014.05.001.

Liu, Y., Sui, Y., Liu, C., Liu, C., Wu, M., Li, B., et al. (2018). A physically crosslinked polydopamine/nanocellulose hydrogel as potential versatile vehicles for drug delivery and wound healing. *Carbohydrate Polymers, 188*, 27–36. https://doi.org/10.1016/j.carbpol.2018.01.093.

Lokanathan, A. R., Uddin, K. M. A., Rojas, O. J., & Laine, J. (2014). Cellulose nanocrystal-mediated synthesis of silver nanoparticles: Role of sulfate groups in nucleation phenomena. *Biomacromolecules, 15*(1), 373–379. https://doi.org/10.1021/bm401613h.

Ma, P., Fu, S., Zhai, H., Law, K., & Daneault, C. (2012). Influence of TEMPO-mediated oxidation on the lignin of thermomechanical pulp. *Bioresource Technology, 118*, 607–610. https://doi.org/10.1016/j.biortech.2012.05.037.

Mishra, S. P., Manent, A. S., Chabot, B., & Daneault, C. (2012). Production of nanocellulose from native cellulose—Various options utilizing ultrasound. *BioResources, 7*(1), 422–435.

Mondal, S. (2017). Preparation, properties and applications of nanocellulosic materials. *Carbohydrate Polymers, 163*, 301–316. https://doi.org/10.1016/j.carbpol.2016.12.050.

Moon, R. J., Martini, A., Nairn, J., Simonsen, J., & Youngblood, J. (2011). Cellulose nanomaterials review: Structure, properties and nanocomposites. *Chemical Society Reviews, 40*(7), 3941–3994. https://doi.org/10.1039/c0cs00108b.

Moreira-Vilar, F. C., Siqueira-Soares, R. D. C., Finger-Teixeira, A., De Oliveira, D. M., Ferro, A. P., Da Rocha, G. J., et al. (2014). The acetyl bromide method is faster, simpler and presents best recovery of lignin in different herbaceous tissues than klason and thioglycolic acid methods. *PLoS One, 9*(10), https://doi.org/10.1371/journal.pone.0110000.

Nascimento, S. A., & Rezende, C. A. (2018). Combined approaches to obtain cellulose nanocrystals, nanofibrils and fermentable sugars from elephant grass. *Carbohydrate Polymers, 180*, 38–45. https://doi.org/10.1016/j.carbpol.2017.09.099.

Pääkko, M., Ankerfors, M., Kosonen, H., Nykänen, A., Ahola, S., Österberg, M., et al. (2007). Enzymatic hydrolysis combined with mechanical shearing and high-pressure homogenization for nanoscale cellulose fibrils and strong gels. *Biomacromolecules, 8*(6), 1934–1941. https://doi.org/10.1021/bm061215p.

Poonguzhali, R., Khaleel Basha, S., & Sugantha Kumari, V. (2018). Synthesis of alginate/nanocellulose bionanocomposite for in vitro delivery of ampicillin. *Polymer Bulletin, 75*(9), 4165–4173. https://doi.org/10.1007/s00289-017-2253-2.

Rahimi, A., Azarpira, A., Kim, H., Ralph, J., & Stahl, S. S. (2013). Chemoselective metal-free aerobic alcohol oxidation in lignin. *Journal of the American Chemical Society, 135*(17), 6415–6418. https://doi.org/10.1021/ja401793n.

Rajala, S., Siponkoski, T., Sarlin, E., Mettänen, M., Vuoriluoto, M., Pammo, A., et al. (2016). Cellulose nanofibril film as a piezoelectric sensor material. *ACS Applied Materials & Interfaces, 8*(24), 15607–15614. https://doi.org/10.1021/acsami.6b03597.

Rezende, C. A., De Lima, M., Maziero, P., Deazevedo, E., Garcia, W., & Polikarpov, I. (2011). Chemical and morphological characterization of sugarcane bagasse submitted to a delignification process for enhanced enzymatic digestibility. *Biotechnology for Biofuels, 4*, 54. https://doi.org/10.1186/1754-6834-4-54.

Rubin, E. M., Himmel, M. E., Ding, S., Johnson, D. K., & Adney, W. S. (2007). Biomass recalcitrance. *Nature, 315*, 804–807. https://doi.org/10.1126/science.1137016.

Sain, M., Pan, Y., Xiao, H., Farnood, R., & Faruk, O. (2013). Development of lignin and nanocellulose enhanced bio PU foams for automotive parts. *Journal of Polymers and the Environment, 22*(3), 279–288. https://doi.org/10.1007/s10924-013-0631-x.

Saito, T., Kimura, S., Nishiyama, Y., & Isogai, A. (2007). Cellulose nanofibers prepared by TEMPO-mediated oxidation of native cellulose. *Biomacromolecules, 8*(8), 2485–2491. https://doi.org/10.1021/bm0703970.

Segal, C., Creely, J. J., Martin, A. E. J., & Conrad, C. M. (1959). An empirical method for estimating the degree of crystallinity of native cellulose using the X-ray diffractometer. *Textile Research Journal, 29*(10), 786–794.

Siró, I., & Plackett, D. (2010). Microfibrillated cellulose and new nanocomposite materials: A review. *Cellulose, 17*(3), 459–494. https://doi.org/10.1007/s10570-010-9405-y.

Souza, S. F., Mariano, M., De Farias, M. A., & Bernardes, J. S. (2019). Effect of depletion forces on the morphological structure of carboxymethyl cellulose and micro/nano cellulose fiber suspensions. *Journal of Colloid and Interface Science, 538*, 228–236. https://doi.org/10.1016/j.jcis.2018.11.096.

Supramaniam, J., Adnan, R., Mohd Kaus, N. H., & Bushra, R. (2018). Magnetic nanocellulose alginate hydrogel beads as potential drug delivery system. *International*

Journal of Biological Macromolecules, 118, 640–648. https://doi.org/10.1016/j.ijbiomac.2018.06.043.

Teixeira, E., de, M., Bondancia, T. J., Teodoro, K. B. R., Corrêa, A. C., Marconcini, J. M., et al. (2011). Sugarcane bagasse whiskers: Extraction and characterizations. *Industrial Crops and Products, 33*(1), 63–66. https://doi.org/10.1016/j.indcrop.2010.08.009.

Tejado, A., Alam, M. N., Antal, M., Yang, H., & van de Ven, T. G. M. (2012). Energy requirements for the disintegration of cellulose fibers into cellulose nanofibers. *Cellulose, 19*(3), 831–842. https://doi.org/10.1007/s10570-012-9694-4.

Van Hai, L., Zhai, L., Kim, H. C., Kim, J. W., Choi, E. S., & Kim, J. (2018). Cellulose nanofibers isolated by TEMPO-oxidation and aqueous counter collision methods. *Carbohydrate Polymers, 191*, 65–70. https://doi.org/10.1016/j.carbpol.2018.03.008.

Wang, Q. Q., Zhu, J. Y., Gleisner, R., Kuster, T. A., Baxa, U., & McNeil, S. E. (2012). Morphological development of cellulose fibrils of a bleached eucalyptus pulp by mechanical fibrillation. *Cellulose, 19*(5), 1631–1643. https://doi.org/10.1007/s10570-012-9745-x.

Wicklein, B., Kocjan, A., Salazar-Alvarez, G., Carosio, F., Camino, G., Antonietti, M., et al. (2015). Thermally insulating and fire-retardant lightweight anisotropic foams based on nanocellulose and graphene oxide. *Nature Nanotechnology, 10*(3), 277–283. https://doi.org/10.1038/nnano.2014.248.

Yue, Y., Han, J., Han, G., Zhang, Q., French, A. D., & Wu, Q. (2015). Characterization of cellulose I/II hybrid fibers isolated from energycane bagasse during the delignification process: Morphology, crystallinity and percentage estimation. *Carbohydrate Polymers, 133*, 438–447. https://doi.org/10.1016/j.carbpol.2015.07.058.

Zhou, Y., Saito, T., Bergström, L., & Isogai, A. (2018). Acid-free preparation of cellulose nanocrystals by TEMPO oxidation and subsequent cavitation. *Biomacromolecules, 19*(2), 633–639. https://doi.org/10.1021/acs.biomac.7b01730.

Zimmermann, T., Pöhler, E., & Geiger, T. (2004). Cellulose fibrils for polymer reinforcement. *Advanced Engineering Materials, 6*(9), 754–761. https://doi.org/10.1002/adem.200400097.